Stapled beta-hairpins featuring 4-mercaptoproline

Jennifer R. Pace, Bryan J. Lampkin, Charles Abakah, Adam Moyer, Jiayuan Miao, Kirsten Deprey, Robert A. Cerulli, Yu-Shan Lin, James D. Baleja, David Baker, and Joshua A. Kritzer*

Supporting Information Placeholder

ABSTRACT: Peptides constrained by intramolecular cross-links, especially stapled α-helices, have emerged as versatile scaffolds for drug development. However, there are fewer examples of similarly constrained scaffolds for other secondary structures. Here, we used a novel computational strategy to identify an optimal staple for antiparallel β-strands, and then we incorporated that staple within a β-hairpin peptide. The hairpin uses 4-mercaptoproline as a novel staple component, which contributes to a unique, kinked structure. The stapled hairpins show a high degree of structure in aqueous solution, excellent resistance to degradation in cell lysates, and cytosolic penetration at micromolar concentrations. They also overlay with a unique subset of kinked hairpin motifs at protein-protein interaction interfaces. Thus, these scaffolds represent promising starting points for developing inhibitors of cellular protein-protein interactions.

Constrained peptides are a rich source of protein ligands, often binding protein surfaces with high affinity and specificity.[1,2] Many of the methods used to discover constrained peptides have difficulties incorporating non-proteinogenic amino acids and chemical cross-links. Computational design could be a more direct route to advanced scaffolds for drug development. However, prior design efforts have struggled to incorporate non-proteinogenic amino acids and cross-links.[3,4] Here, we describe the computational design of β-hairpins organized by four non-proteinogenic amino acids. The hairpins are further stabilized by a novel intramolecular cross-link (a "staple") involving the conformationally constrained amino acid 4-mercaptoproline (4MP). The designed β-hairpins are well-structured in aqueous solution, resist degradation in cell lysates, and penetrate the cytosol of cultured cells at micromolar concentrations.

Previously, several groups have employed cysteine alkylation using *ortho*-, *meta*- and *para*-dibromomethylbenzene, the "CLIPS" reaction pioneered by Timmerman and colleagues,[5] to stabilize loop and α-helical structures.[6–10] Cysteine, D-cysteine, homocysteine, and penicillamine have all been incorporated into structure-stabilizing staples using this chemistry. We envisioned using the same chemistry to staple 4MP (Fig. 1a). 4MP is a hydroxyproline analog that was previously applied to native chemical ligation and studies of proline conformation,[11–14] but not to peptide stapling. Using 4MP for stapling is appealing for several reasons, including the increased torsional rigidity of 4MP relative to cysteine, and the potential to use up to four different stereoisomers (all commercially available and synthetically accessible)[13] to vary staple geometry.

Given the prominent role of proline in stabilizing β-turns,[15,16] we turned to β-hairpin peptides as a model system to evaluate 4MP-based staples. **HP7** is one of the smallest well-structured β-hairpins, and its truncated analog **ΔHP7** is less well-structured because it lacks two stabilizing charge pairs (Fig. 1b).[15] **ΔHP7** and **HP7** have been used previously to test the structural effects of β-hairpin modifications.[17] Our initial strategy employed diversity-oriented stapling guided by simple modeling: we substituted (*2S,4R*)-4MP directly for proline within **ΔHP7**, then produced analogs with the 4MP stapled to cysteine substituted at one of two nearby positions (Table S1). *Bis*-thiol alkylation with *ortho*-, *meta*-, and *para*-dibromomethylbenzene was performed on fully deprotected, unpurified peptides as described,[5,6] with near-quantitative yields. These results demonstrate that 4MP is fully compatible with stapling unprotected peptides in solution. The secondary structures of the peptides were analyzed by circular dichroism (CD) spectroscopy (Fig. S6). These peptides ranged in the extent of their β-hairpin structure, but none were more well-structured than the parent peptide **ΔHP7**. The most well-structured, **ΔHP7-GC-p**, had a positive Cotton effect of 8,900 near 228 nm, implying roughly half the level of structure of parent peptide **ΔHP7** (Fig 1b,c).

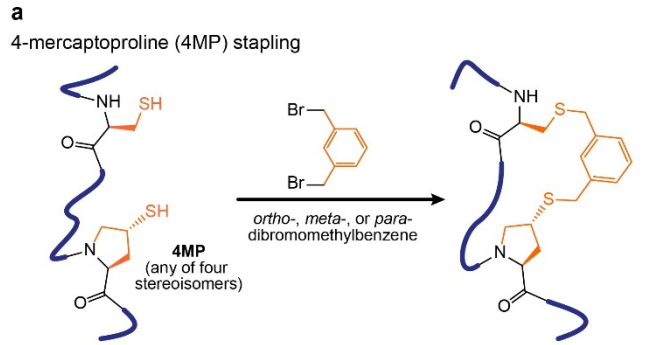

b

Name	Sequence	Termini	Staple	Degree of structure	T_{50}
ΔHP7	TWNPATGKWT	capped	none	0.61	31.9
ΔHP7-GC-p	TWN4ATCKWT	capped	*para*	0.33	n/m
Δ4MP-a	TWyCTpXG4GWT	capped	allyl	0.63	28.4
Δ4MP-m	TWyCTpXG4GWT	capped	*meta*	0.86	32.1
HP7	KTWNPATGKWTE	free	none	1.0	58.7
4MP-a	KTWyCTpXG4GWTE	free	allyl	1.26	50.8
4MP-m	KTWyCTpXG4GWTE	free	*meta*	1.41	58.5

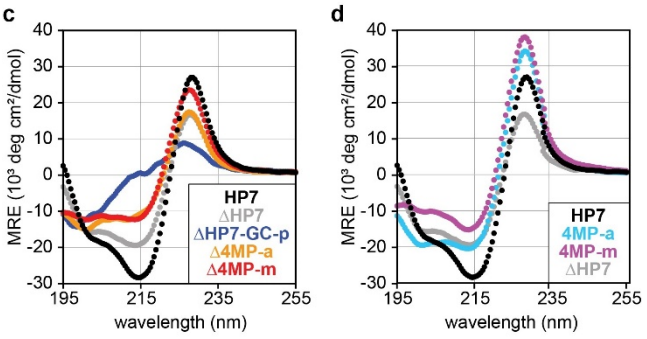

Figure 1. Stapled peptides with 4-mercaptoproline with β-hairpin structure. (a) Peptide stapling using thiol alkylation with 4-mercaptoproline (4MP). (b) Hairpin peptides analyzed by circular dichroism (CD) spectroscopy. The predicted β-turn within each sequence is underlined. Lowercase letters denote D-amino acids, X denotes 1-aminocyclopropane-1-carboxylic acid, and 4 denotes (*2S,4R*)-4-mercaptoproline. Degree of structure is calculated from the Trp-Trp exciton coupling band at 228 nm. Degree of structure is reported relative to **HP7**, and T_{50} values represent the temperature at which each peptide was observed to retain 50% structure (Fig. S7-S8); n/m denotes value not measured. (c) CD spectra for **HP7**, **ΔHP7**, **ΔHP7-GC-p** (initial design), **Δ4MP-a** (computational design, unstapled), and **Δ4MP-m** (computational design, stapled). (d) CD spectra for **HP7**, **ΔHP7**, **4MP-a** (computational design, unstapled), and **4MP-m** (computational design, stapled). CD data shown are the average of three independent trials.

We next sought to apply a more systematic design approach. However, prior large-scale computational design approaches could not be applied to 4MP stapling due to the diversity of possible staple geometries and the non-proteinogenic nature of 4MP. Thus, prior approaches designed scaffolds with well-folded secondary structure, then grafted disulfide bonds onto the already-designed scaffold (Fig. 2a).[4] In this work, we took a novel approach. We systematically modeled many different staples to find those most compatible with a specific secondary structure, and then the rest of the peptide was grafted onto the designed staple (Fig 2b). We started by systematically identifying which combinations of residues and cross-linker would fulfill the hydrogen bonding geometry of antiparallel β-strands. Conformers were generated for all possible permutations of 4MP (*2S,4R* and *2S,4S* stereoisomers), cross-linker (*ortho-*, *meta-*, and *para*-dimethylbenzene, alkyl chains, and disulfides), and second thiol-containing residue (cysteine and homocysteine) using RDKit (Fig. S1-S2).[18] 10,000 conformers for each permutation were generated and subsequently energy-minimized using AIMNet(SMD)-D4.[19,20] By evaluating the energies of each conformational ensemble, we identified which staples were most compatible with antiparallel β-strands (Fig. S2-S4, Fig. 2b Step 1). Next, we attached the stapled strands to 29 different, crystallographically verified β-turns. A turn containing D-Pro and 1-aminocyclopropane-1-carboxylic acid (Acpc)[21,22] was the only β-turn which templated two amide bonds between residues 1 and 4 of the β-turn, which superimposed closely with the stapled strands. Grafting the D-Pro-Acpc turn onto the stapled strands produced a stapled β-turn (Fig. 2b Step 2). Finally, we sought to introduce the stapled β-turn into the model sequence **HP7**, but simple substitution was complicated by the 4MP residue which disrupted the canonical β-hairpin structure. We compared models with different L- and D-amino acids on the strand opposite the 4MP, and we observed that a D-amino acid allowed extension of the β-hairpin (Fig. 2b Step 3). The complete β-hairpin was assembled by superimposing the stapled β-strands, the β-turn, the D-amino acid, and the antiparallel β-strands from **HP7**. Side chains for the final design, **4MP-m**, were selected for torsional compatibility with the template (D-Tyr4, Thr6, Gly9, and Gly11), or to match model β-hairpin **HP7** (residues 1-3 and 12-14).

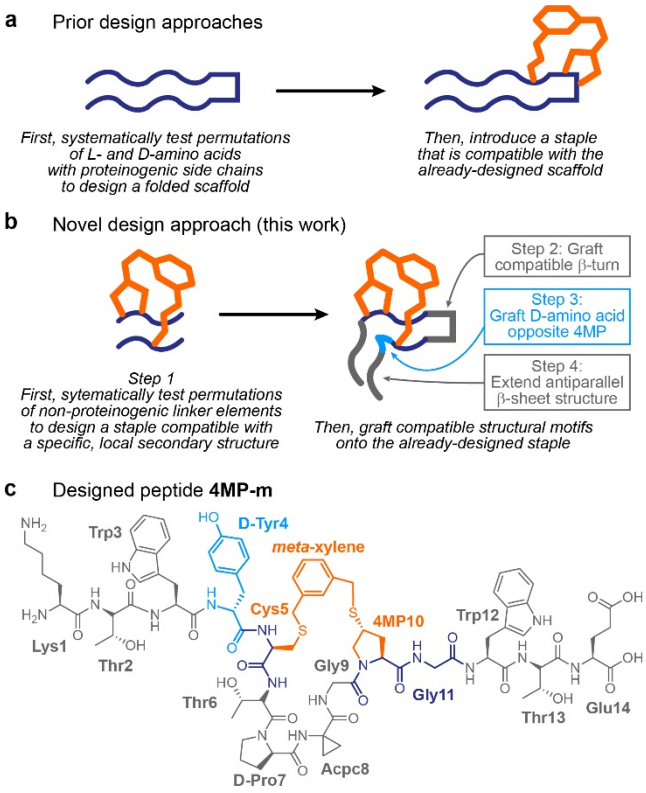

Figure 2. Computational design of β-hairpins stapled with 4-mercaptoproline. (a) Prior design approaches grafted a staple onto an already-designed scaffold. (b) The novel approach described here employed a systematic search for staples that were compatible with the target structure (antiparallel β-strands), and then grafted compatible structural motifs onto the already-designed staple. (c) Chemical structure of designed peptide **4MP-m**, with structural elements colored as in (b).

We synthesized **4MP-m** and its unstapled analog **4MP-a**, which was alkylated with allyl bromide instead of a bifunctional cross-linker. These were compared to parent β-hairpin **HP7** using CD spectroscopy (Fig. 1d). **4MP-a** and **4MP-m** both had the same overall CD signature as **HP7**, with characteristic minimum at 215 nm indicating β-sheet structure and a strong maximum at 228 nm from exciton coupling of cross-strand Trp side chains.[23] Due to the incorporation of multiple non-natural amino acids, including D-amino acids, we used the strength of the Trp-Trp exciton coupling as an indicator of extent of β-hairpin structure. **4MP-a** had a 26% more intense Cotton effect near 228 nm compared to **HP7**, suggesting that the non-proteinogenic amino acids in the unstapled analog (D-Tyr, D-Pro, Acpc, and 4MP) increased the extent of β-hairpin structure at room temperature. **4MP-m** had a 41% more intense Cotton effect near 228 nm compared to **HP7**, suggesting that adding the staple increased the extent of β-hairpin structure even further. These results indicated that the non-proteinogenic amino acids supported robust β-hairpin structure that was fully compatible with the novel 4MP staple.

To examine the relative roles of the staple and the β-turn, we prepared analogs of **4MP-a** and **4MP-m** with either of the turn residues D-proline or Acpc substituted with glycine (Fig. S7). These analogs had reduced hairpin structure relative to **4MP-a** and **4MP-m**. Also, unlike **4MP-m**, analogs with altered β-turns had less hairpin structure when stapled. These results indicated cooperativity between the designed staple and the β-turn.

To see if the designed features could stabilize β-hairpin structure within the shorter peptide **ΔHP7**, we prepared the corresponding analogs **Δ4MP-a** and **Δ4MP-m** and compared them to **ΔHP7** using CD spectroscopy. The unstapled analog **Δ4MP-a** had a Cotton effect at 228 nm with similar intensity to that of **ΔHP7**, and the stapled analog **Δ4MP-m** had an intensity 41% greater than that of **ΔHP7** (Fig. 1c), further suggesting the designed staple promotes β-hairpin structure.

We used CD thermal melts to compare the thermodynamic stability of the designed hairpins and analogs. T_{50} values of for **HP7**, **4MP-a**, and **4MP-m** were 58.7°C, 50.8°C, and 58.5°C, respectively, and similar trends were observed for the truncated analogs **ΔHP7**, **Δ4MP-a**, and **Δ4MP-m**. These data indicated that, despite being more well-structured at room temperature, the stapled peptides do not have significantly different thermal stability. van't Hoff analysis revealed that, compared to **HP7** and **ΔHP7**, unstapled analogs **4MP-a** and **Δ4MP-a** had greater enthalpic contributions to folding. Also, the stapled analogs had a smaller entropic barrier to folding than their corresponding unstapled analogs (Fig. S11-S12, Table S3). Further, the analogs with glycine substitutions in the β-turn lost favorable enthalpic contributions to folding relative to **4MP-m**, further indicating cooperativity between the designed staple and the β-turn. These data are consistent with the design strategy.

Next, we used NMR spectroscopy to examine the aqueous solution structure of **4MP-m** at higher resolution. We identified 56 NOEs between non-consecutive residues, including many cross-strand interactions (Fig. 3a and Table S5). These NOEs were used to constrain customized simulated annealing simulations that included molecular dynamics in explicit water.[24] These simulations produced an ensemble with a low-energy cluster that was consistent with 92% of the observed NOEs (Fig. 3b) and no violations greater than 0.6 Å (Table S5). Comparing the lowest-energy structure of this cluster to the predicted structure resulted in a backbone RMSD of 0.91 Å, and the major difference was the type I′ β-turn at residues 7 and 8 instead of the type II′ β-turn that was predicted (Fig. S18). As an independent measure of extent of structure and intramolecular hydrogen bond formation, we performed variable-temperature NMR experiments (Fig. S16, Table S6). We observed protected chemical shifts consistent with hydrogen bond formation for the amide protons of D-Tyr4, Thr6, Gly9, and Gly11 (Fig. 3c). These data are fully consistent with the results from CD and from NOE-guided simulated annealing. All together, these data indicated that, in aqueous solution, **4MP-m** adopts a unique, kinked structure in which the 4MP staple and the D-Tyr residues position the β-turn roughly perpendicular to the rest of the β-hairpin.

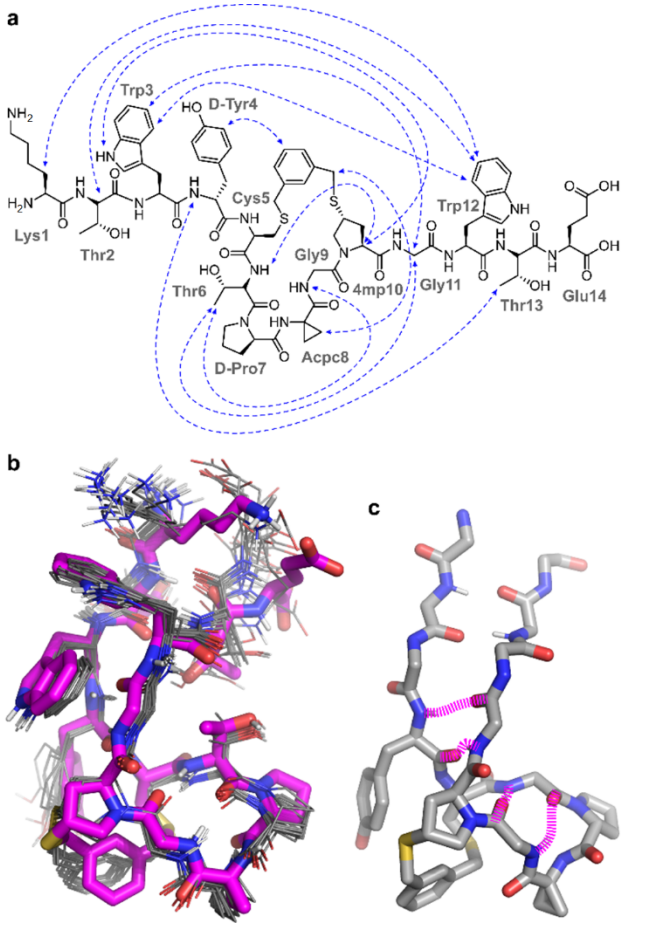

Figure 3. 3D structure of 4MP-m in aqueous solution. (a) Chemical structure of **4MP-m** with selected medium-range NOEs shown as blue double-headed arrows. Complete NOEs are shown in Table S6. (b) Predicted structure of **4MP-m** (magenta) overlaid with a low-energy cluster of 12 structures derived from simulated annealing (gray lines). (c) Lowest-energy calculated solution structure of **4MP-m**. Side chains not involved in the kinked turn are omitted. Magenta dotted lines indicate hydrogen bonding independently supported by variable temperature NMR data (Fig. S16 and Table S6).

One of the potential advantages of incorporating non-proteinogenic amino acids and covalent staples is resistance to proteolytic degradation. To test whether the designed β-hairpins were stable to degradation, we adapted a cell lysate stability assay recently applied for development of olefin-stapled α-helices.[25–27] Because HeLa cell lysate contains all cellular

proteases including lysosomal proteases, this represents a relatively rigorous test for metabolic stability of peptide therapeutics. Control peptides **HP7** and **ΔHP7** were degraded rapidly, with roughly 0% and 19%, respectively, remaining after only two hours (Fig. 4a). Few discrete degradation products of these peptides were detected by mass spectrometry. **4MP-a** and **4MP-m**, the unstapled and stapled analogs of **HP7**, were also degraded relatively rapidly (roughly 22% and 7%, respectively, remaining after 4 hours). However, even after 24 hours in HeLa cell lysate, the primary degradation products for **4MP-a** and **4MP-m** were intact except for the two N-terminal amino acids. The truncated analogs **Δ4MP-a** and **Δ4MP-m** were much more stable to degradation in cell lysates, with calculated half-lives of 30 and 21 hours, respectively. No sulfide oxidation was observed for any hairpin peptides, even after 24 hours of incubation with cell lysates.

Another sought-after property for constrained peptide scaffolds is the ability to penetrate cells and localize to the cytosol.[28,29] While cytosolic penetration depends greatly on identity of side chains, some constrained peptides (such as olefin-stapled α-helices) represent privileged scaffolds that can be engineered for cytosolic penetration, while some others (such as lactam-stapled peptides) are rarely observed to be cell-penetrant.[28,29] Thus, it was unclear whether stapled β-hairpins represented a scaffold with measurable cytosolic penetration. We examined the extent to which stabilized β-hairpins penetrate the cytosol using the recently reported Chloroalkane Penetration Assay (CAPA).[30,31] We produced hairpin peptides with chloroalkane tags on their N-termini and measured their cytosolic penetration after a 4-hour incubation using CAPA (Fig. 4b). Surprisingly, chloroalkane-tagged versions of **HP7** and **ΔHP7** had CP_{50} values of 4.7 and 0.9 μM, respectively. These data could be confounded by degradation.[31] The less degradation-prone **4MP-a** and **4MP-m** showed essentially no cytosolic localization when incubated with cells up to 20 μM. By contrast, chloroalkane-tagged **Δ4MP-a** and **Δ4MP-m** had CP_{50} values of 5.4 and 9.6 μM, respectively, indicating substantial cytosolic penetration after only 4 hours at these concentrations. Notably, these are only two- to three-fold higher than the analogous CP_{50} value for Tat (3.1 μM),[30] demonstrating that these stapled hairpins have a moderate ability to penetrate to the cytosol. We also observed no signs of toxicity for any peptide up to 30 μM, as measured by the proportion of live cells in each sample when gating for CAPA.[31] Overall, the CAPA data indicated that the stapled β-hairpin was more cell-penetrant when it was smaller in size and had fewer charges. This observation matches prior work on stapled α-helices.[32,33] Moving forward, these scaffolds will allow us to examine whether the biophysical properties known to promote cytosolic localization and bioactivity for stapled α-helices[32,33] will apply in the context of stapled β-hairpins, considering they are similar in size and physicochemical properties.[34–37]

Relative to previous work in the field,[3,4] this work provides novel computational methodology that can be applied to any staple and any secondary structure. The designed β-hairpins **4MP-m** and **Δ4MP-m** display a high degree of structure, matching or exceeding the level of structure observed for previously described β-hairpins based on **HP7** and **ΔHP7**.[15,17] In fact, the small temperature dependences of the chemical shifts of D-Tyr4 and Gly9 amide protons are within the range typically observed for the folded core of globular proteins.[38,39] The kinked structure of **4MP-m** is unique compared to **HP7** and other model β-hairpins (Fig. S19).[15–17,23] To assess whether the kinked hairpin mimics protein-like structures, we aligned the backbone of **4MP-m** with all possible 12-residue fragments in a non-redundant subset of the Protein Data Bank. We found many close alignments, including numerous hairpins at protein-protein interfaces (Table S7, Fig. S20-S21). These results indicate that **4MP-m** and related hairpins will be useful starting points for the design of unique protein-protein interaction inhibitors.

In this work, we also demonstrate the versatility of 4MP as a novel component of structure-stabilizing staples. While we employed the (*2S,4R*) and (*2S,4S*) stereoisomers, we anticipate the other two stereoisomers will be equally useful as building blocks for peptide stapling, especially as analogs of D-proline. Proline and D-proline are key structure-promoting residues for β-hairpins, but also for many other secondary structures including other β-turn-nucleated loops, α-helix caps, polyproline helices, and collagen-like helices and assemblies.[40–42] Additionally, a computationally designed set of over 200 well-structured head-to-tail cyclic peptides was previously reported, and over 98% of these cyclic peptides had one or more prolines or D-prolines.[3] Overall, we anticipate that the application of 4MP staples to these and other structures will provide straightforward ways to generate highly structured cyclic and multicyclic peptides, spanning many diverse structural classes and providing unique scaffolds for drug development.

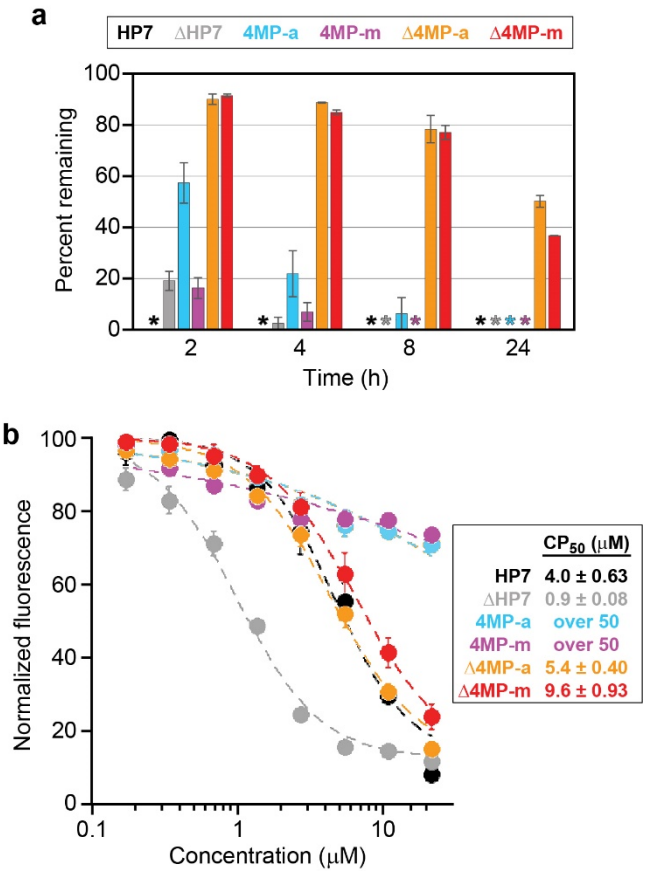

Figure 4. Biological degradation and cytosolic penetration of designed β-hairpins. (a) β-hairpin peptides were incubated for selected time points in HeLa cell lysate at 37 °C. Enzymatic reactions were quenched by adding methanol and supernatants were analyzed by analytical HPLC. Areas under each peptide chromatogram peak were normalized to the area under the zero timepoint chromatogram peak. Average values and standard errors of the mean were calculated from three

independent replicates. Asterisks indicate zero or near-zero values. (b) Cytosolic penetration of chloroalkane-tagged peptides as measured by the chloroalkane penetration assay.[30,31] Error bars denote standard errors of the mean from three independent replicates. Curves (dotted lines) were fitted and CP_{50} values were calculated as described.[30,31]

ASSOCIATED CONTENT

Supporting Information

Experimental and computational methods, information on peptide synthesis and characterization, additional CD data and thermal melts, NMR data sets including variable temperature experiments, simulated annealing methodology, and PDB alignment methodology and results.

AUTHOR INFORMATION

Corresponding Author

Joshua A. Kritzer – Department of Chemistry, Tufts University, Medford, MA 02155, United States; Email: joshua.kritzer@tufts.edu

Authors

Jennifer R. Pace – Department of Chemistry, Tufts University, Medford, MA 02155, United States; Present address: Department of Chemistry, St. Anselm College, Manchester, NH 03102, United States;
Bryan J. Lampkin – Department of Chemistry, Tufts University, Medford MA 02155, United States;
Charles Abakah – Department of Chemistry, Tufts University, Medford, MA 02155, United States;
Adam Moyer – Molecular Engineering and Sciences Institute, University of Washington, Seattle WA 98195, United States;
Jiayuan Miao – Department of Chemistry, Tufts University, Medford, MA 02155, United States;
Kirsten Deprey – Department of Chemistry, Tufts University, Medford, MA 02155, United States;
Robert A. Cerulli – Cell, Molecular and Developmental Biology Program, Graduate School of Biomedical Sciences, Tufts University, Boston, MA 02111, United States;
Yu-Shan Lin – Department of Chemistry, Tufts University, Medford, MA 02155, United States;
James D. Baleja – Graduate School of Biomedical Sciences, Tufts University, Boston, MA 02111, United States;
David Baker – Department of Biochemistry, Institute for Protein Design, and Howard Hughes Medical Institute, University of Washington, Seattle, WA 98195, United States;
Joshua A. Kritzer – Department of Chemistry, Tufts University, Medford, MA 02155, United States.

Notes

The authors declare no competing financial interests.

ACKNOWLEDGMENTS

This work was supported by NIH GM125856 and NSF 2003010, Ruth L. Kirschstein Individual Predoctoral NRSA Fellowship F30CA220678 to R.A.C., and NIH GM124160. The work used NMR instrumentation that was purchased with funding from NIH grant S10OD020073.

REFERENCES

(1) Guarracino, D. A.; Riordan, J. A.; Barreto, G. M.; Oldfield, A. L.; Kouba, C. M.; Agrinsoni, D. Macrocyclic Control in Helix Mimetics. *Chem. Rev.* **2019**, *119* (17), 9915–9949.

(2) Hill, T. A.; Shepherd, N. E.; Diness, F.; Fairlie, D. P. Constraining Cyclic Peptides To Mimic Protein Structure Motifs. *Angew. Chem. Int. Ed.* **2014**, *53*, 2–24.

(3) Hosseinzadeh, P.; Bhardwaj, G.; Mulligan, V. K.; Shortridge, M. D.; Craven, T. W.; Pardo-Avila, F.; Rettie, S. A.; Kim, D. E.; Silva, D.-A.; Ibrahim, Y. M.; Webb, I. K.; Cort, J. R.; Adkins, J. N.; Varani, G.; Baker, D. Comprehensive Computational Design of Ordered Peptide Macrocycles. *Science* **2017**, *358* (6369), 1461–1466.

(4) Bhardwaj, G.; Mulligan, V. K.; Bahl, C. D.; Gilmore, J. M.; Harvey, P. J.; Cheneval, O.; Buchko, G. W.; Pulavarti, S. V. S. R. K.; Kaas, Q.; Eletsky, A.; Huang, P.-S.; Johnsen, W. A.; Greisen, P. J.; Rocklin, G. J.; Song, Y.; Linsky, T. W.; Watkins, A.; Rettie, S. A.; Xu, X.; Carter, L. P.; Bonneau, R.; Olson, J. M.; Coutsias, E.; Correnti, C. E.; Szyperski, T.; Craik, D. J.; Baker, D. Accurate de Novo Design of Hyperstable Constrained Peptides. *Nature* **2016**, *538* (7625), 329–335.

(5) Timmerman, P.; Beld, J.; Puijk, W. C.; Meloen, R. H. Rapid and Quantitative Cyclization of Multiple Peptide Loops onto Synthetic Scaffolds for Structural Mimicry of Protein Surfaces. *ChemBioChem* **2005**, *6* (5), 821–824.

(6) Peraro, L.; Siegert, T. R.; Kritzer, J. A. Conformational Restriction of Peptides Using Dithiol Bis-Alkylation. *Meth. Enzymol.* **2016**, *580*, 303–332.

(7) Heinis, C.; Rutherford, T.; Freund, S.; Winter, G. Phage-Encoded Combinatorial Chemical Libraries Based on Bicyclic Peptides. *Nature Chemical Biology* **2009**, *5* (7), 502–507.

(8) Jo, H.; Meinhardt, N.; Wu, Y.; Kulkarni, S.; Hu, X.; Low, K. E.; Davies, P. L.; DeGrado, W. F.; Greenbaum, D. C. Development of α-Helical Calpain Probes by Mimicking a Natural Protein–Protein Interaction. *J. Am. Chem. Soc.* **2012**, *134* (42), 17704–17713.

(9) Siegert, T. R.; Bird, M. J.; Makwana, K. M.; Kritzer, J. A. Analysis of Loops That Mediate Protein–Protein Interactions and Translation into Submicromolar Inhibitors. *J. Am. Chem. Soc.* **2016**, *138* (39), 12876–12884.

(10) Peraro, L.; Zou, Z.; Makwana, K. M.; Cummings, A. E.; Ball, H. L.; Yu, H.; Lin, Y.-S.; Levine, B.; Kritzer, J. A. Diversity-Oriented Stapling Yields Intrinsically Cell-Penetrant Inducers of Autophagy. *J. Am. Chem. Soc.* **2017**, *139* (23), 7792–7802.

(11) Cadamuro, S. A.; Reichold, R.; Kusebauch, U.; Musiol, H.-J.; Renner, C.; Tavan, P.; Moroder, L. Conformational Properties of 4-Mercaptoproline and Related Derivatives. *Angew. Chem. Int. Ed.* **2008**, *47* (11), 2143–2146.

(12) Costantini, N. V.; Ganguly, H. K.; Martin, M. I.; Wenzell, N. A.; Yap, G. P. A.; Zondlo, N. J. The Distinct Conformational Landscapes of 4S-Substituted Prolines That Promote an Endo Ring Pucker. *Chem.-Eur. J.* **2019**, *25* (48), 11356–11364.

(13) Pandey, A. K.; Naduthambi, D.; Thomas, K. M.; Zondlo, N. J. Proline Editing: A General and Practical Approach to the Synthesis of Functionally and Structurally Diverse Peptides. Analysis of Steric versus Stereoelectronic Effects of 4-Substituted Prolines on Conformation within Peptides. *J. Am. Chem. Soc.* **2013**, *135* (11), 4333–4363.

(14) Gui, Y.; Qiu, L.; Li, Y.; Li, H.; Dong, S. Internal Activation of Peptidyl Prolyl Thioesters in Native Chemical Ligation. *J. Am. Chem. Soc.* **2016**, *138* (14), 4890–4899.

(15) Andersen, N. H.; Olsen, K. A.; Fesinmeyer, R. M.; Tan, X.; Hudson, F. M.; Eidenschink, L. A.; Farazi, S. R. Minimization and Optimization of Designed β-Hairpin Folds. *J. Am. Chem. Soc.* **2006**, *128* (18), 6101–6110.

(16) Hughes, R. M.; Waters, M. L. Model Systems for Beta-Hairpins and Beta-Sheets. *Curr. Opin. Struct. Biol.* **2006**, *16* (4), 514–524.

(17) Sawyer, N.; Arora, P. S. Hydrogen Bond Surrogate Stabilization of β-Hairpins. *ACS Chem. Biol.* **2018**, *13* (8), 2027–2032.

(18) Riniker, S.; Landrum, G. A. Better Informed Distance Geometry: Using What We Know To Improve Conformation Generation. *J. Chem. Inf. Model.* **2015**, *55* (12), 2562–2574.

(19) Zubatyuk, R.; Smith, J. S.; Leszczynski, J.; Isayev, O. Accurate and Transferable Multitask Prediction of Chemical Properties

with an Atoms-in-Molecules Neural Network. *Science Advances* **2019**, *5* (8), eaav6490.

(20) Caldeweyher, E.; Ehlert, S.; Hansen, A.; Neugebauer, H.; Spicher, S.; Bannwarth, C.; Grimme, S. A Generally Applicable Atomic-Charge Dependent London Dispersion Correction. *J. Chem. Phys.* **2019**, *150* (15), 154122.

(21) Diener, M. E.; Metrano, A. J.; Kusano, S.; Miller, S. J. Enantioselective Synthesis of 3-Arylquinazolin-4(3H)-Ones via Peptide-Catalyzed Atroposelective Bromination. *J. Am. Chem. Soc.* **2015**, *137* (38), 12369–12377.

(22) Hurtley, A. E.; Stone, E. A.; Metrano, A. J.; Miller, S. J. Desymmetrization of Diarylmethylamido Bis(Phenols) through Peptide-Catalyzed Bromination: Enantiodivergence as a Consequence of a 2 Amu Alteration at an Achiral Residue within the Catalyst. *J Org Chem* **2017**, *82* (21), 11326–11336.

(23) Wu, L.; McElheny, D.; Takekiyo, T.; Keiderling, T. A. Geometry and Efficacy of Cross-Strand Trp/Trp, Trp/Tyr, and Tyr/Tyr Aromatic Interaction in a β-Hairpin Peptide. *Biochemistry* **2010**, *49* (22), 4705–4714.

(24) Cummings, A. E.; Miao, J.; Slough, D. P.; McHugh, S. M.; Kritzer, J. A.; Lin, Y.-S. β-Branched Amino Acids Stabilize Specific Conformations of Cyclic Hexapeptides. *Biophys. J.* **2019**, *116* (3), 433–444.

(25) Partridge, A. W.; Kaan, H. Y. K.; Juang, Y.-C.; Sadruddin, A.; Lim, S.; Brown, C. J.; Ng, S.; Thean, D.; Ferrer, F.; Johannes, C.; Yuen, T. Y.; Kannan, S.; Aronica, P.; Tan, Y. S.; Pradhan, M. R.; Verma, C. S.; Hochman, J.; Chen, S.; Wan, H.; Ha, S.; Sherborne, B.; Lane, D. P.; Sawyer, T. K. Incorporation of Putative Helix-Breaking Amino Acids in the Design of Novel Stapled Peptides: Exploring Biophysical and Cellular Permeability Properties. *Molecules* **2019**, *24* (12), 2292.

(26) Cerulli, R. A.; Shehaj, L.; Tosic, I.; Jiang, K.; Wang, J.; Frank, D. A.; Kritzer, J. A. Cytosolic Delivery of Peptidic STAT3 SH2 Domain Inhibitors. *Bioorganic & Medicinal Chemistry* **2020**, *28* (12), 115542.

(27) Cerulli, R. A.; Shehaj, L.; Brown, H. F.; Pace, J. R.; Mei, Y.; Kritzer, J. A. Stapled Peptide Inhibitors of Autophagy Adapter LC3B. *ChemBioChem* **2020**, *21* (19), 2777–2785.

(28) Dougherty, P. G.; Sahni, A.; Pei, D. Understanding Cell Penetration of Cyclic Peptides. *Chem. Rev.* **2019**, *119* (17), 10241–10287.

(29) Peraro, L.; Kritzer, J. A. Emerging Methods and Design Principles for Cell-Penetrant Peptides. *Angew. Chem.-Int. Edit.* **2018**, *57* (37), 11868–11881. https://doi.org/10.1002/anie.201801361.

(30) Peraro, L.; Deprey, K. L.; Moser, M. K.; Zou, Z.; Ball, H. L.; Levine, B.; Kritzer, J. A. Cell Penetration Profiling Using the Chloroalkane Penetration Assay. *J. Am. Chem. Soc.* **2018**, *140* (36), 11360–11369.

(31) Deprey, K.; Kritzer, J. A. Quantitative Measurement of Cytosolic Penetration Using the Chloroalkane Penetration Assay. *Meth. Enzymol.* **2020**, *641*, 277–309.

(32) Bird, G. H.; Mazzola, E.; Opoku-Nsiah, K.; Lammert, M. A.; Godes, M.; Neuberg, D. S.; Walensky, L. D. Biophysical Determinants for Cellular Uptake of Hydrocarbon-Stapled Peptide Helices. *Nat. Chem. Biol.* **2016**, *12* (10), 845–852.

(33) Chu, Q.; Moellering, R. E.; Hilinski, G. J.; Kim, Y.-W.; Grossmann, T. N.; Yeh, J. T.-H.; Verdine, G. L. Towards Understanding Cell Penetration by Stapled Peptides. *Med. Chem. Commun.* **2015**, *6* (1), 111–119.

(34) Fouche, M.; Schafer, M.; Berghausen, J.; Desrayaud, S.; Blatter, M.; Piechon, P.; Dix, I.; Martin Garcia, A.; Roth, H.-J. Design and Development of a Cyclic Decapeptide Scaffold with Suitable Properties for Bioavailability and Oral Exposure. *ChemMedChem* **2016**, *11* (10), 1048–1059.

(35) Tian, Y.; Zeng, X.; Li, J.; Jiang, Y.; Zhao, H.; Wang, D.; Huang, X.; Li, Z. Achieving Enhanced Cell Penetration of Short Conformationally Constrained Peptides through Amphiphilicity Tuning. *Chem. Sci.* **2017**, *8* (11), 7576–7581.

(36) Safa, N.; Anderson, J. C.; Vaithiyanathan, M.; Pettigrew, J. H.; Pappas, G. A.; Liu, D.; Gauthier, T. J.; Melvin, A. T. CPProtectides: Rapid Uptake of Well-Folded Beta-Hairpin Peptides with Enhanced Resistance to Intracellular Degradation. *Pept. Sci.* **2019**, *111* (2), e24092.

(37) Miller, S. E.; Schneider, J. P. The Effect of Turn Residues on the Folding and Cell-Penetrating Activity of Beta-Hairpin Peptides and Applications toward Protein Delivery. *Pept. Sci.* **2020**, *112* (1), e24125.

(38) Baxter, N. J.; Williamson, M. P. Temperature Dependence of 1H Chemical Shifts in Proteins. *J Biomol NMR* **1997**, *9* (4), 359–369. https://doi.org/10.1023/A:1018334207887.

(39) Cierpicki, T.; Otlewski, J. Amide Proton Temperature Coefficients as Hydrogen Bond Indicators in Proteins. *J Biomol NMR* **2001**, *21* (3), 249–261.

(40) Shoulders, M. D.; Raines, R. T. Collagen Structure and Stability. *Annu. Rev. Biochem.* **2009**, *78*, 929–958.

(41) Gavenonis, J.; Sheneman, B. A.; Siegert, T. R.; Eshelman, M. R.; Kritzer, J. A. Comprehensive Analysis of Loops at Protein-Protein Interfaces for Macrocycle Design. *Nat Chem Biol* **2014**, *10* (9), 716–722.

(42) Maison, W.; Arce, E.; Renold, P.; Kennedy, R. J.; Kemp, D. S. Optimal N-Caps for N-Terminal Helical Templates: Effects of Changes in H-Bonding Efficiency and Charge. *J. Am. Chem. Soc.* **2001**, *123* (42), 10245–10254.

Table of Contents artwork